Electric Vehicle Power Propulsion System Control Based on Time-Varying Fractional Calculus: Implementation and Experimental Results

Mohammad-Hassan Khooban, *Senior Member, IEEE*, Meysam Gheisarnezhad, Navid Vafamand, and Jalil Boudjadar

Abstract: **Nowadays, due to the fact that motor efficiency is strictly related to the diminution of emissions, researchers pay much attention to find a robust and efficient motor control technique for Hybrid Electric Vehicles (HEVs). In this study, an optimal type-2 fuzzy fractional P + ID (IT2FOFP+ID) controller is applied to solve the throttle position and speed control problem of the HEVs. It is undeniable that the performance and effectiveness of the fuzzy-based PID controllers are depended on its gains' value. Hence, a novel improved heuristic technique, called IJAYA algorithm, is employed for the online tuning of the coefficients embedded in the specific controller structure. In contrast with the classical control methodologies that suffer from the lack of the self-regulating feature, the established controller has been adjusted on-line automatically. As another advantage of this control strategy, it is a model-free scheme and does not need the mathematical computational to identify the system model. To appraise the supremacy of the optimal IT2FOFP+ID controller than the other prevalent methodologies, a highly nonlinear EV model is utilized as a case study. In addition, the usefulness and robustness of the proposed method are tested by the experimental data, the EPA New York City Cycle (NYCC). In the end, the new time-varying proposed technique is validated and implemented in hardware-in-the-loop (HiL) real-time simulation based on OPAL-RT to study the feasibility of the designed IT2FP+ID controller with check outcomes on a physical platform**.

KeyWords: **DC Motor Speed Control, Improved JAYA (IJAYA) algorithm, Type-2 Fuzzy Fractional P + ID (IT2FOFP+ID) controller.**

I: INTRODUCTION

DUE to the shortages of fossil fuel reserves, environmental emission, increasing costs of electric transportation, Hybrid Electric Vehicles (HEVs) has become an emerging trend [1-3]. HEVs can potentially offer great benefits including smooth operation, high energy efficiency, safety improvement and energy security [4, 5]. In addition, the whole HEVs produce zero tailpipe emissions, which reduce local air pollution especially when they are widely used in urban areas. Owing to the above excellent properties, it is anticipated that the future automotive industry will be dominated by the HEVs. One of the key ingredients for the establishment of an HEV system is the control mechanism. Since such systems have the time-variant nature, the conventional deterministic methodologies are not resilient enough to ensure the excellent performance for both the dynamic and steady-state requirements.

M. H. Khooban and J. Boudjadar are with the Department of Engineering, Aarhus University Denmark. (e-mail: mhkhoban@gmail.com, jalil@eng.au.dk).

M. Gheisarnezhad is with Department of Electrical Engineering, Najafabad Branch, Islamic Azad University, Isfahan, Iran (e-mail: m.ghesar2@gmail.com).

N. Vafamand is with the School of Electrical and Computer Engineering, Shiraz University (e-mail: n.vafamand@shirazu.ac.ir).

Various intelligent/advanced control methodologies are addressed in the literature in the speed issue of the HEVs [6, 7]. For instance, a fuzzy logic oriented by sliding mode scheme is suggested in [8] for the speed regulation of the non-linear EVs. The hybrid scheme mainly concentrated on reducing the negative effects of the chattering phenomenon in the non-linear system. In [9], the non-integer controllers are effectively accommodated in a cascade control loop as the primary and supplementary regulators (controllers) for the real-time speed control of a highly non-linear HEV. The real-time responses yielded by [9] have proved that the non-integer controller handles the dynamic variations excellently; however, the experimental aspects of the concerned HEV system has not been investigated in the work. The authors of [10] proposed a robust control methodology using the MPC and fuzzy model (with the Takagi–Sugeno type) for the speed tracking of EVs. Although the control strategy, which was introduced in [10], demonstrated satisfactory performance against various examined operating conditions, the sophisticated scheme is not applicable in the practical applications due to its very rich mathematical design. To overcome the computational complexity, an optimal free-model controller is implemented in [11] for controlling the operation of the EVs using a combination of the general type-2 fuzzy system and PI controller. Since the suggested scheme, in this paper, does not require the mathematical modeling of the EVs it is straightforward to be practically applied. Besides, large numbers of papers are studied, in the literature, in the context of the EVs control such as adaptive control [12], Reinforcement Learning [13], Multi-Agent system [14] and neural network [15].

Recently, the integration of the PI/PID controller and fuzzy logic in the suitable configurations is gaining recognition as a potent tool in the control theory. The benefit of the cooperative scheme is its capability to deal with the nonlinear systems and when their mathematical models are complex to get. Generally, type-1 fuzzy logic controllers (T1FLCs) are known as a proper choice for control of problems that there is not enough information about the system dynamic. Up to now, various structures of FLC based PID controllers, with the aim of achieving a more desirable robust control mechanism than the PID controllers, were investigated by researchers for resistance to the complex problems [16, 17]. Their comparative analysis reveals that the application of the FLCs ameliorates the closed loop performance of the PI/PID controllers to tackle high degrees of complexities (e.g. non-linearity and uncertainty) by the online setting of the controller coefficients. In spite of the successes of T1FLCs, they are less effective against linguistic uncertainties, which are included in unstructured environments. Owing to the limitations of the

T1FLCs to handle such uncertainties, the type-2 fuzzy sets (T2FSs) are introduced since their membership functions (MFs) are also fuzzy [18]. Three-dimensional MFs are used to characterize the T2FSs, which offer a higher degree of freedom over the T1FSs with two-dimensional MFs. Therefore, T2FLCs can be employed in cases where the conditions are too uncertain to find membership grades accurately.

Nowadays, due to the flexibility and high robustness of the non-integer (fractional-order (FO)) PID controllers, control engineers have tended to benefit from fractional-order calculus than integer ones [19, 20]. After the effective application of the FO-PID controllers, exhaustive efforts have been conducted by many contemporary control engineers to attain a higher level of robustness feature than the conventional FLCs (or T1FLCs) by integrating the FLCs with non-integer based approaches. For example, various decomposed combination configurations of the FLC based non-integer controllers with their related comparative merits were studied in [21] for three classes of the oscillatory non-integer plants. Meanwhile, a novel structure of the non-integer fuzzy PID controller is introduced in [22] to handle two different processes including a non-linear plant and an open loop unstable plant. It is noted that the enhanced flexibility in the design of the controller coefficients causes the complexity in adjusting these coefficients. As a result, a large number of papers have presented several optimization approaches to tune the coefficients of FO-based controllers. In [23], a combination of cooperative of FLC with non-integer differ-integral operators is established and cuckoo search (CS) algorithm has been used to design the coefficients embedded before and after the FLC. More recently, a Fuzzy Fractional Order PI+I controller is, maidenly, studied in [24], where the particle swarm optimization (PSO) technique was formulated for optimal setting of the specific controller coefficients. According to the above literature review, the non-integer PID controllers were developed by hybridizing with T1FLCs; therefore, its extension with the IT2FLCs will offer a new research field for scientific communities in the context of T2FSs. This fact encouraged authors to think on the line of establishing the IT2FLCs based non-integer PID controllers for the plants with high inherent non-linearity [25, 26].

Form the literature survey, it is disclosed that most of the earlier research adopted the model-based methodologies in the engineering problems; however, these schemes suffer the need for the model identification. To put it in another way, in order to establish these schemes for the speed control of the HEV, an accurate mathematical model of the HEV system is needed. Hence, according to the complex and severe nonlinear dynamic behaviors of the HEV systems, obtaining an accurate model for such systems, in reality, is very difficult or maybe impossible. In order to solve this difficulty, utilizing a robust and adaptive model-free controller for the control problem of the power propulsion system of HEVs can be a good way. The model-free controllers, which have been established for the speed control problem in the context of HEVs, can be included as fuzzy logic, model-free reinforcement learning, and neural network, wavelet transforms [15, 27]. However, these techniques are not robust over the aforesaid complexity of the HEV systems.

The approach suggested in this work is an expansion of the non-integer controller to the model-free control problem and invokes a new robust control design scheme for manipulating the electronic throttle control system (ETCS) of the HEV to regulate the throttle position, which can be then deployed in the power management of the propulsion system to controller the HEV speed. It is shown that the power of the HEV electric motor is affected by the throttle position. Thereby, the throttle poison acts as an actuator for the HEV speed. Thus, a new optimal IT2FOFP+ID controller is proposed in this study, which is a development of the non-integer order calculus on T2FSs. Moreover, in order to have an optimal and time-varying control approach, an improved version of JAYA algorithm is applied for the optimal setting of the suggested intelligent adaptive controller. Finally, by establishing the suggested model-free framework on the OPAL-RT hardware, the feasibility of the numerical analysis in a physical platform is validated. Briefly, the contributions of this work are listed as:

(i) Given the fact that the conventional fuzzy systems are not able to directly overcome uncertainties, in this work, T2FSs has been utilized to handle parametric uncertainties.

(ii) Owing to the two additional degrees of freedom in non-integer PID controllers, they can better regulate the dynamical attributes of a control system. So, a hybrid proposed controller in this paper can effectively handle the uncertainties and disturbances over conventional controllers.

(iii) The suggested control efforts are only based on the accessible system input/output information and can be obtained online.

(iv) The proposed model-free controller can be applied to a vast variety of industrial control system applications without any complexity.

(v) Qualitative appraisal of both theoretical and experimental outcomes reveals a reasonable agreement between simulated and experimental results.

The paper is organized as follows. The mathematical problem formulation and dynamic model of the nonlinear HEV are described in Section II. The implementation of the suggested model-free controller is presented in Section III. In Section IV, a brief outline of the original JAYA along with the enhanced version of the JAYA algorithm is drawn. Also, the concerned objective function for the optimal setting of the controller coefficients is given in this section. In Section V, the experimental setup is described followed by the performance comparison of the IT2FOFP+ID, IT2FP+ID and MPC controllers for speed profile trajectory tracking against the non-linearity and parametric uncertainty. Finally, the conclusions of the suggested work are given in Section VI.

II: HYBRID ELECTRIC VEHICLE MODELLING

In this section, the dynamic model of the concerned HEV system is presented. This will be used in the next sections to regulate the vehicle speed to the desired value. The main parts of the HEVs can include the electrical and mechanical sections. Particularly, vehicle dynamics are related to the mechanical part while the ETCS is related to the electrical part [9]. In order to keep the desired speed of HEV, the angular throttle position of the vehicle should be regulated. Fig. 1(a) depicts the overall dynamic model of the HEV system. In the

This article has been accepted for publication in a future issue of this journal, but has not been fully edited. Content may change prior to final publication. Citation information: DOI 10.1109/TIV.2019.2904415, IEEE Transactions on Intelligent Vehicles

following, each part of the HEV will be discussed and analyzed carefully.

A. The Modelling of ETCS

In order to spin the throttle plate based on the desired angle ($0 < \theta < \frac{\pi}{2}$), a DC servo motor (DCSM) is utilized in this study as the ETCS. In addition, for controlling the DCSM, an armature voltage (E_a) is used [9]. Fig. 1(b) is provided to illustrate the corresponding electro-mechanical structure.

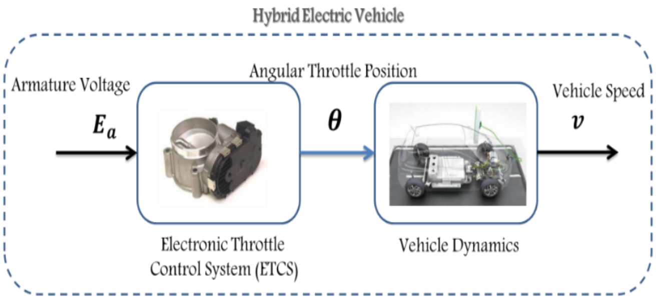

Fig. 1(a). The overall structure of the HEV(s)

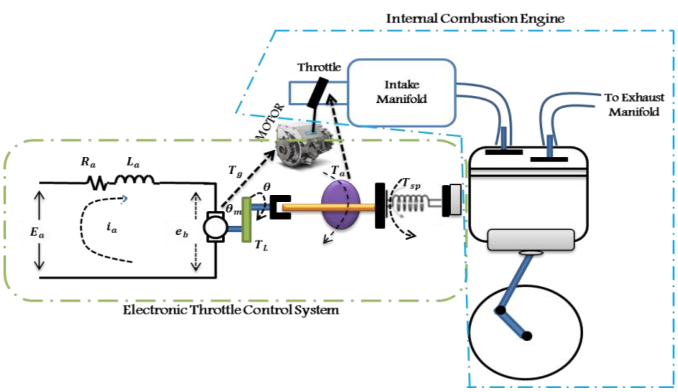

Fig. 1(b). The structure of the ETCS in HEVs

Now, the nonlinear system state of the ETCS can be written as follows [9]:

$$\begin{bmatrix} \dot{\theta} \\ \frac{d\dot{\theta}}{dt} \\ \dot{i_a} \end{bmatrix} = \begin{bmatrix} 0 & 1 & 0 \\ \frac{-K_{sp}}{J} & \frac{-K_f}{J} & \frac{NK_t}{J} \\ 0 & \frac{NK_b}{L_a} & \frac{-R_a}{L_a} \end{bmatrix} \begin{bmatrix} \theta \\ \frac{d\theta}{dt} \\ i_a \end{bmatrix} + \begin{bmatrix} 0 \\ \frac{-K_{sp}}{J} - \frac{R_p^2 R_{af}\pi}{J} \Delta P Cos^2\theta \\ 0 \end{bmatrix} + \begin{bmatrix} 0 \\ 0 \\ \frac{1}{L_a} \end{bmatrix} u \tag{1}$$

where K_{sp} introduces the throttle spring constant, N is the gear ratio, K_t shows the motor torque constant, K_b is the back emf constant, L_a is the armature inductance and R_a denotes the armature resistance. In (1), R_p is considered as the throttle plate radius as well as R_{af} is treated as the focal point of air flow on the plate. In addition, $J = N^2 J_m + J_g$, K_f=$(N^2 b_m + b_t)$ and ΔP=$(P_{atm} - P_m)$. For the detailed mathematical modelling equations of the ETSC, the readers are referred to [11].

B. The Model of Nonlinear Vehicle Dynamic

In Fig. 1.c, the nonlinear vehicle model of EVs is shown. According to Fig. 1.c, the modeling of the vehicle consists of the balance among the forces acting on a running vehicle i.e. road load and the traction force. The EV moves with a speed V, have mass m and up the slope of angle β. F_e is assumed as the propulsion force for the HEV to whirl forward. It is noted that F_e should dominate the road load force $F_{road\ load}$ and the gravity induced force F_g. Based on the second law of Newton, the model of the nonlinear HEVs is mathematically expressed as follows [9, 28]:

$$\begin{aligned} m\frac{dv}{dt} &= F_e(\theta) - F_{road\ load} - F_g \\ \tau_e \frac{dF_e(\theta)}{dt} &= -F_e(\theta) + F_{e1}(\theta) \end{aligned} \tag{2}$$

where the time constant of the engine reaction is shown by τ_e as well as $F_{e1}(\theta)$ can be written as below:

$$F_{e1}(\theta) = F_i + \gamma\sqrt{\theta} \tag{3}$$

In (3), γ is introduced as a positive value and F_i is denoted as the engine idle power. Now, the function F_g can be expressed by:

$$F_g = mgsin\,(\frac{\beta\pi}{180}) \tag{4}$$

In this step, by the summation of the aerodynamic drag (F_{drag}), rolling resistance (F_{roll}) and the power owing to axle/wheel bearing friction (F_{damp}), $F_{road\ load}$ is calculated as below.

$$F_{road\ load} = F_{drag} + F_{roll} + F_{damp} \tag{5}$$

In (5), the forces F_{drag}, F_{roll}, and F_{damp} can be calculated as below:

$$F_{roll} = \mu_f mgcos(\frac{\beta\pi}{180}) \tag{6}$$

$$F_{drag} = 0.5\rho A_{fr} C_d v^2 sgn(v) \tag{7}$$

where $sgn(.)$ stands for the signum function. Also,

$$F_{damp} = \frac{b_w v}{r_{tire}} \tag{8}$$

By arranging the equations (2–9), the nonlinear vehicle dynamic can be presented as follows [3]:

$$\begin{aligned} m\frac{dv}{dt} = F_i + \gamma\sqrt{\theta} - \tau_e \frac{dF_e(\theta)}{dt} \\ - \mu_f mgcos\left(\frac{\beta\pi}{180}\right) \\ - 0.5\rho A_{fr} C_d v^2 sgn(v) - \frac{b_w v}{r_{tire}} \\ - mgsin\,(\frac{\beta\pi}{180}) \end{aligned} \tag{9}$$

In table I, the value of the parameters of the HEV is presented. The overall HEV system is obtained by augmenting (1) and (9) with the output and input defined in (1). The goal is to propose a novel intelligent controller to control the speed of the overall HEV by the means of manipulating the throttle position. As it can be seen in (2), the HEV speed v is affected by the nonlinear function of the throttle position (i.e. $\sqrt{\theta}$). So, controlling of the throttle position is tightly related with that of the HEV speed.

This article has been accepted for publication in a future issue of this journal, but has not been fully edited. Content may change prior to final publication. Citation information: DOI 10.1109/TIV.2019.2904415, IEEE Transactions on Intelligent Vehicles

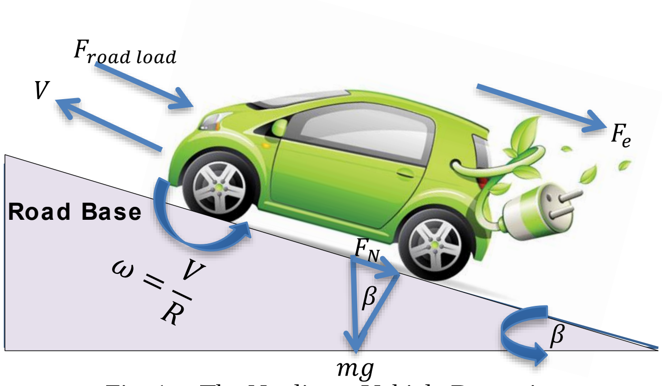

Fig. 1.c. The Nonlinear Vehicle Dynamic

Table I: The HEV system's parameters [9]

Symbol	Value	Symbol	Value	Symbol	Value
$b_m\ (N\ ms/rad)$	0.03	$J_g\ (Kg\ m^2)$	0.005	$R_a\ (\Omega)$	1.9
$J_m\ (Kg\ m^2)$	0.001	$\rho\ (Kg/m^3)$	1.25	$R_{af}\ (m)$	0.002
$b_t\ (N\ ms/rad)$	0.003397	$L_a\ (mH)$	0.003	$R_p\ (m)$	0.0015
$b_w\ (N\ ms/rad)$	0.035	$g\ (m/s^2)$	9.81	$F_i\ (N)$	3000
$K_b(V\ s/rad)$	0.1051	$V\ (Volt)$	0~48	$r_{tire}\ (m)$	0.2794
$K_{sp}\ (N\ m/rad)$	0.4316	$\theta_0\ (rad)$	π/2	μ_f	0.015
$K_t\ (N\ m/A)$	0.1045	$\gamma\ (N)$	12500	$I\ (A)$	78
$\alpha\ (N/(m/s)^2)$	6	$m\ (Kg)$	1767	N	4
$\beta\ (degree)$	0	$\tau_e\ (s)$	0.2	Step size	0.001

III: A NON-INTEGER TYPE-II FUZZY P+ID CONTROLLER

As presented in Section II, the concerned HEV system is made of two subsystems i.e. vehicle dynamics (primary subsystem) and ETCS (secondary subsystem). In this section, a nonlinear non-integer type-2 fuzzy P+ID controller with a model-free and self-adjustable feature is presented to solve the speed control problem of a highly nonlinear HEV system. The proposed controller is an improved approach, which has been previously presented by [26] to control the sophisticated industrial applications.

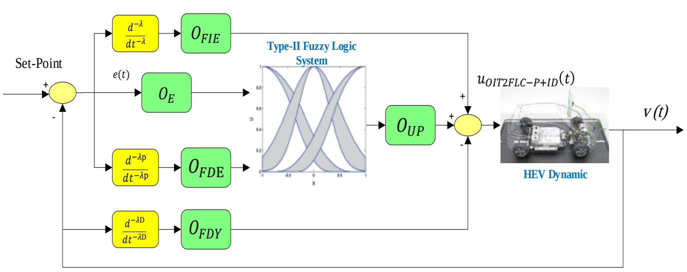

Fig. 2. The general scheme of the model-free IT2FOFP+ID controller.

It is assumed that the IT2FOFP+ID controller, which is modified by substituting the proportional term in the traditional proportional–integral–derivative controller via two inputs fuzzy logic controller, is schemed to modify the control performance in both transient and steady- state response for HEVs. It should be noted that no hardware adaptations are needed for its real-time implementation since the proposed control technique keeps the basic simplicity of the PID controller. In this brief, in order to address the uncertainty problems, which exist in the HEV system, and provide a more effective control method, the suggested controller technique uses the benefits of the fractional order calculus as well as the type-II fuzzy logic theory [11]. The structure of the IT2FOFP+ID controller used in this study is depicted in Fig. 2. As shown in Fig. 2, the established structure is inherited from three components i.e. IT2FLC, fractional order integrator, and fractional order derivative. Inputs to the IT2FLC controller are error and fractional derivative of error and the output of IT2FLC is u_{IT2FLC}. The error is used as the input of a fractional order integrator, while the output is employed as the input of the fractional order derivative. By summing the outputs of the three components, a direct output $u_{IT2FOFP+ID}$ is obtained to regulate the armature voltage.
According to Fig. 2, the following equation can be written as the output of the specific structured controller [26]:

$$u_{OIT2FLC-P+ID}(t) = O_{UP}(U_{IT2FLC}) + O_{FIE}\frac{d^{-\lambda}(e(t))}{dt^{-\lambda}} - O_{FDY}\frac{d^{-\lambda D}(y(t))}{dt^{-\lambda D}} \tag{10}$$

As shown in Fig. 2, the quality of the control actions of the controller are obsoletely depended on the controller parameter values. Therefore, in order to make an adaptive and robust controller over the aforesaid system complexities, a new improved algorithm, entitled IJAYA, is utilized for the online tuning of the smart non-integer controller parameters. Next section is provided to present the design process of the improved optimization algorithm.

IV: OPTIMIZATION ALGORITHM OPTIMIZATION ALGORITHM AND OBJECTIVE FUNCTION

A. Overview of the JAYA algorithm

JAYA is a kind of population-based algorithm coined by Rao [29] and it is free from the prevalent algorithm parameter tuning which makes it unique than other heuristic techniques. In the native algorithm, a candidate search agent is ameliorated through moving towards the global agent (best solution) and getting away from the worst agent at the same time.

JAYA initiates with a random population of the search agents with the size of P (i.e. i=1, 2,..., P) of a D-dimensional vector within the decisive space. Then, a new search agent is determined by the following movement characteristic [29].

$$Y_{i,j}^k = y_{i,j}^k + rand_1\left(y_{j,best}^k - \left|y_{i,j}^k\right|\right) - rand_2\left(y_{j,worst}^k - \left|y_{i,j}^k\right|\right) \tag{11}$$

where $Y_{i,j}^k$ is the updated search agent of $y_{i,j}^k$ during k^{th} generation; $rand_1$ and $rand_2$ are uniform random numbers in [0 1]; $y_{j,best}^k$ and $y_{j,worst}^k$ are the best and worst values reached until the k^{th} generation. The computational procedure for the JAYA technique is sketched Fig. 3.a.

B. Improved JAYA algorithm

B.1. Chaotic extended opposition-based initialization

Based on the idea of opposition-based learning, considering simultaneously a search agent with its opposing can lead to a better candidate search agents. As proved in the literature, an opposite position of a candidate search agent has a higher chance to be near to the global agent [30] than when a candidate search agent is generated in random. In this sub-section, a chaotic extended opposition is established for the efficient initialization in the JAYA.

According to the feature of the extended opposition, a random number is produced within the opposition position of a search agent and the closest lower/upper bound to its opposite number and it is, mathematically, characterized by [31]:

$$\breve{y}_{j,eo} = \begin{cases} rand(\breve{y}_j,\ ub_j), & y_j < (lb_j + ub_j)/2 \\ rand(lb_j,\ \breve{y}_j), & y_j > (lb_j + ub_j)/2 \end{cases} \quad (12)$$

where $j = 1, 2, \dots, D$; lb_j and ub_j are the lower and upper bound for the j^{th} component of each search agent, respectively. $\breve{y}_{eo}$ denotes the extended opposite point of y, and $\breve{y}$ denotes the opposite point of y where $\breve{y}_j = lb_j + ub_j - y_j$.

In order to enhance the diversity of a search agent, a chaotic version of the extended opposition, instead of its randomness approach, is introduced and incorporated in the algorithm initialization phase. In this study, the chaotic sequences are generated by a well-known logistic map as defined below [32].

$$x^k = 4\,x^{k-1}(1 - x^{k-1}) \quad (13)$$

where x^k is the k^{th} chaotic number distributed in the range [0 1], while x^0 must not be 0, 0.25, 0.5, 0.75 or 1.

The procedure computation of the JAYA

```
Initialize the parameters Max-Gen, P and D
for i=1 to P  do
    for j=1 to D
        y_{i,j} = lb_j + rand * (ub_j - lb_j);
    end for
end for
  while gen=1 to Max-Gen do
    for i=1 to P do
      Identify the best and worst solutions in the population
      Update the solutions by the Eq. (12)
    end for
  Check limitations and repair the solutions
  if they are violated from boundary constraints
      for i=1 to P  do
        if f(Y_i) < f(y_i) then
          Replace y_i with Y_i
        end if
      end for
      Report the optimum solution
  end while
```

Fig. 3(a). The pseudo-code of the original JAYA algorithm.

B.2. Enhanced global searching based firefly algorithm

According to the scheme adopted in JAYA, the distance between the best and worst agents is a deciding factor in providing the diversification of the whole search agents during the iterative process. Depending on the specific distance, in the native algorithm, causes the search agents to encounter the diversity loss when converges to the best agent in the final iterations and subsequently leads to the premature convergence.

The procedure computation of the IJAYA

```
Initialize the parameters Max-Gen, P, D and α
for i=1 to P  do
    for j=1 to D
        y_{i,j} = lb_j + rand * (ub_j - lb_j);
    end for
end for
for i=1 to P  do
    for j=1 to D  do
        C_{i,j} = (lb_j + ub_j )/2;
        Randomly initialize chaos variables x_j^0 ϵ(0 1)
        if (y_{i,j} < C_{i,j})  then
          y̆_{i,j}^{eo} = y̆_{i,j} + 4 x_j^{k-1}(1 - x_j^{k-1})(ub_j - y̆_{i,j});
        else
          y̆_{i,j}^{eo} = lb_j + 4 x_j^{k-1} (1 - x_j^{k-1}) (y̆_{i,j} - lb_j);
        end if
    end for
end for
Select P fittest individuals from set of {y_{i,j}, y̆_{i,j}^{eo} } as the initial population.
  while gen=1 to Max-Gen do
    for i=1 to P do
      Identify the best and worst solutions in the population
      if rand < 1/2 then
        Update the solutions by the original JAYA algorithm
      else
        Calculate r_{gx} and r_{wx} using Eqs. (16) and (17)
        Update the solutions by the Eq. (15)
      end if
    end for
Check limitations and repair the solutions if they are violated from boundary constraints
      for i=1 to P  do
        if f(Y_i) < f(y_i) then
          Replace y_i with Y_i
        end if
      end for
      Report the optimum solution
  end while
      Report the optimum solution
end while
```

Fig. 3(b). The pseudo-code of the proposed algorithm.

In order to keep diversity along with a fast convergence specification, the updating mechanism of the JAYA is improved by hybridizing with the firefly algorithm (FA) [33]. Based on this strategy, the search agents are modified by the original JAYA with a probability 0.5; otherwise, they are proposed as follows:

$$\begin{aligned} Y_{i,j}^k = y_{i,j}^k &+ rand_1\, e^{-r_{gx}^2}\left(y_{j,best}^k - \left|y_{i,j}^k\right|\right) \\ &- rand_2\, e^{-r_{wx}^2}\left(y_{j,worst}^k - \left|y_{i,j}^k\right|\right) \\ &+ \alpha\,(\psi - 1/2) \end{aligned} \quad (14)$$

where α is a user-selected scaling factor, ψ is a random number in [0 1], $r_{gx} = \sqrt{\sum_{j=1}^{D}(y_{j,best} - y_{i,j})^2}$ and $r_{wx} = \sqrt{\sum_{j=1}^{D}(y_{j,worst} - y_{i,j})^2}$ are the euclidean distance between

This article has been accepted for publication in a future issue of this journal, but has not been fully edited. Content may change prior to final publication. Citation information: DOI 10.1109/TIV.2019.2904415, IEEE Transactions on Intelligent Vehicles

$\{y_{i,j},\ y^{k}_{j,best}\}$, $\{y_{i,j},\ y^{k}_{j,worst}\}$. The pseudo-code of the suggested IJAYA algorithm is shown in Fig. 3(b).

Now, by applying the proposed optimization algorithm for time-varying adjusting the coefficients of the suggested controller, the non-integer type-II fuzzy logic P+ID controller can properly handle the non-linearity and parametric uncertainty. Next section is provided to validate the superiority of the suggested optimal time-varying control over the existing controllers (e.g. MPC and conventional optimal type-II fuzzy logic P+ID controller). Totally, the heuristic techniques (e.g. PSO, Genetic, Bat and CS) do not require any data about the system anymore. In simpler terms, the population-based methodologies only require to formulate the fitness function for the guidance of its search. Consequently, this study uses the following cost function for finding the best value of the controller's parameters.

$$E(k) = {}^{1}/_{N} \sum_{i=1}^{N} |e(i)| + |\Delta\omega(i)| \tag{15}$$

where $e(i)$ introduces the trajectory error of the i^{th} sample for the object as well as N shows the number of samples, i defines the iteration number and $\Delta\omega(i)$ is the speed changes.

Remark 1: The proposed approach is model-free and can be applied to any HEV systems. The proposed approach uses the JAYA algorithm to online update the gains of the controller parameter values. In section V, it is shown that the proposed approach can be applied to throttle position-based HEVs and power converter-based ones.

V: SIMULATION and EXPERIMENTAL RESULTS

In this section, for verification of the performance and efficiency of the suggested control method, a highly nonlinear hybrid electric vehicle, which is represented in Fig. 1(b), is simulated in MATLAB/Simulink software. Each control approach requires to be evaluated in the real-time simulator before its execution on the industrial application. Consequently, an OPAL-RT emulator is applied, in this work, to explore the applicability yielded by the suggested control technique in a real-time testbed. The real-time HiL method is used to emulate errors and delays that do not exist in the classical off-line simulations and to ascertain that the proposed controller has the capability of running in real-time without overruns. Fig. 4 illustrates the layout of the HIL setup on a Real-Time Simulator (RTS).

The main parts of the setup are as [34, 35]:

1) OPAL-RT as an RTS which simulates the concerned HEV system;

2) A PC as the command station (programming host) in which the Matlab/Simulink based code will be executed on the OPAL-RT;

3) A router as connector all the setup elements in the same sub-network. Also, the OPAL-RT is linked to DK60 board through Ethernet ports.

Moreover, in order to affirm the supremacy and acceptability of the suggested optimal IT2FOFP+ID controller, a comparison is made between the proposed control technique and other famous and powerful controllers like MPC and conventional optimal IT2FP+ID controller.

Scenario 1: Real-world driving test conditions based on the EPA New York City Cycle (NYCC) is applied in this real-time simulation to appraise the robustness and usefulness of the suggested time-varying non-integer control approach.

The profile of the NYCC is represented in Fig. 5(a). Now, the result of the implemented robust non-integer controller on the HEV model, which is presented in Fig. 1(b), based on OPAL-RT real-time simulation is depicted in Fig. 5(a). Also, the control signal and the error signal of the proposed method over the MPC and conventional optimal type-II fuzzy logic P+ID controller are illustrated in Figs. 5(b) and (c).

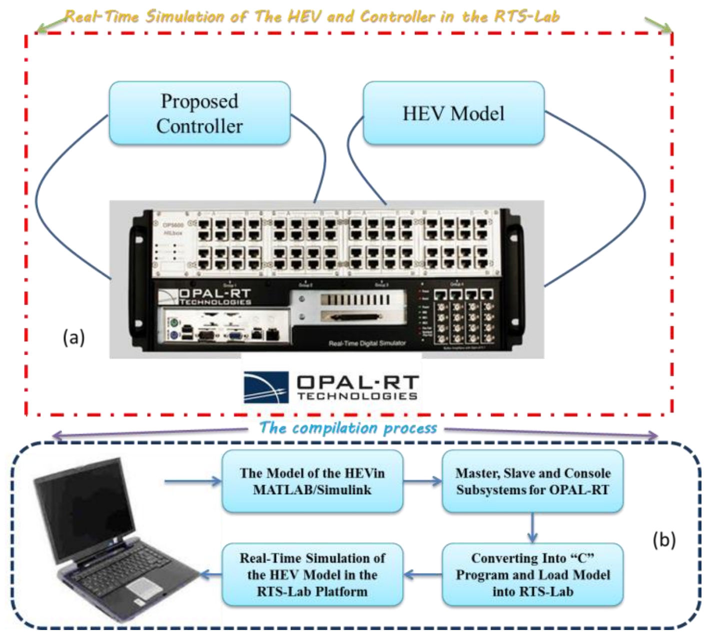

Fig. 4. The Real-time experimental setup.

Based on the control and error signals, which were presented in Figs. 5(b) and (c), it is obvious that the optimal proposed technique has less error signal over the other controllers. This can be a good proof that the suggested controller in this paper, which has implemented in the OPAL-RT, has superior performance than the fuzzy MPC [36] with prediction horizon 3 incorporated by Takagi-Sugeno (T-S) model [37, 38] and conventional optimal type-II fuzzy logic P+ID controllers. In addition, the control signal is presented in Fig. 5.c to indicate the band-limited control signal.

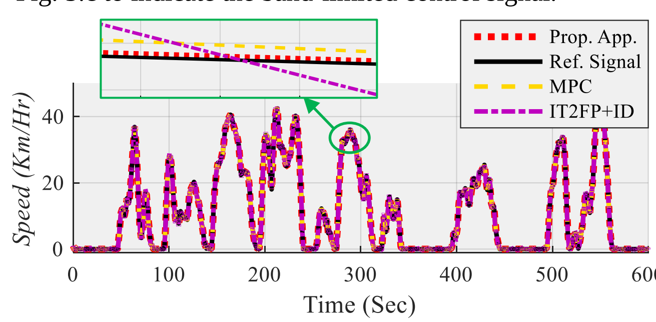

Fig. 5(a). Performance of suggested Controllers, IT2FP+ID and MPC to track the NYCC Speed Test reference signal.

This article has been accepted for publication in a future issue of this journal, but has not been fully edited. Content may change prior to final publication. Citation information: DOI 10.1109/TIV.2019.2904415, IEEE Transactions on Intelligent Vehicles

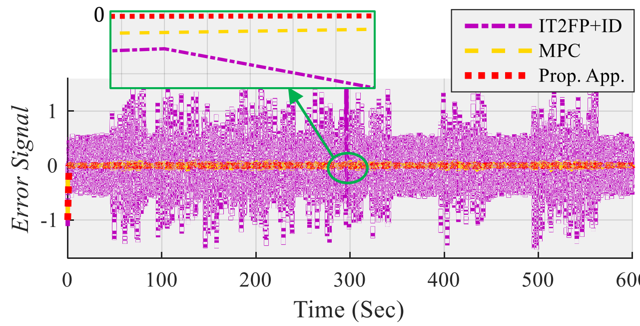

Fig. 5(b). The error signal of suggested Controllers, IT2FP+ID and MPC to track NYCC Speed Test.

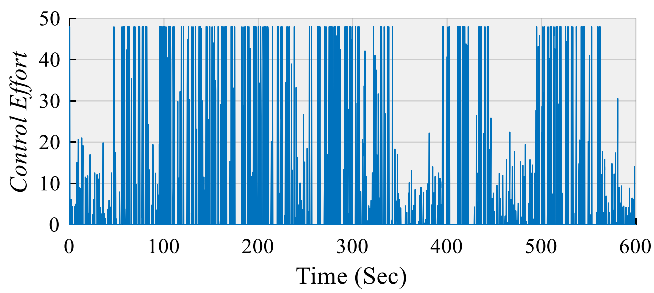

Fig. 5(c). The control signal of suggested Controllers to track NYCC Speed Test.

<u>Scenario 2</u>: This subsection is provided to more challenge the robustness and performance of the non-integer suggested controller over the structural uncertainties [39, 42]. Therefore, in order to access the IT2FOFP+ID controller performance over the HEV system's parameter variations, Table II is considered for the HEV model uncertainties. In a simple word, the percentage of change in the parameters of the HEV model is shown in Table II. In the following, the outcomes of the simulation of the proposed method over the MPC and the conventional type-2 fuzzy P+ID controllers are shown in Fig. 6(a). Furthermore, the error signal and the control effort of the IT2FOFP+ID, MPC, and IT2FP+ID are presented in Figs. 6(b) and (c).

It is undeniable that overshoots are one of the most important factors, which should be considered in the designed controllers. Once more, it can be easily understood from the simulation results shown in Figs. 6.a-c that the suggested non-integer controller highly meliorates performance as compared to other controller structures, especially when the overshoots and settling time are concerned. Also, in spite of the variations considered in the HEV model parameters in scenario 2, the IT2FOFP+ID controller approach outperforms the other two, as depicted in Fig. 6(a).

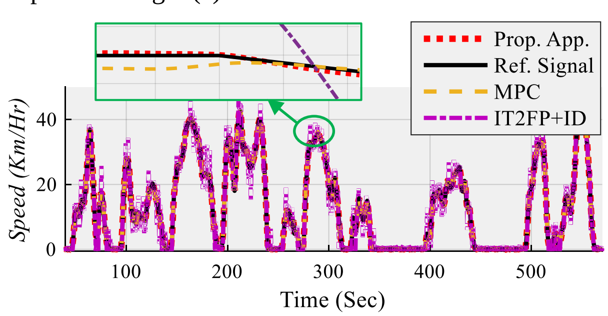

Fig. 6(a). Performance of suggested Controllers, IT2FP+ID and MPC to track NYCC Speed Test.

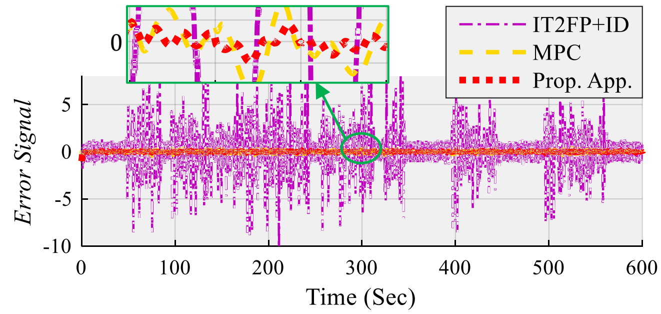

Fig. 6(b). Error signal of suggested Controllers, IT2FP+ID and MPC to track NYCC Speed Test.

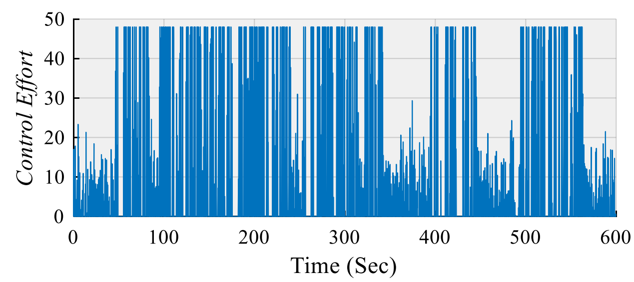

Fig. 6(c). The control signal of suggested Controller to track NYCC Speed Test.

Figs. 6(a)-(c) reveal the robustness of the IT2FOFP+ID controller approach over the various coefficients changes. Besides, the control signal and the error signal, which were presented in Figs. 6(b) and (c) prove that the suggested structured controller has better accuracy and efficiency against the MPC and the IT2FP+ID controllers.

Table II. Uncertain Parameters of HEV

Parameters	Variation Range
	Scenario 1
$\Delta R = R_a + R_f$ (Ω)	-40%
$\Delta L = L_a + L_f$ (mH)	+30%
r_e (m)	+20%
J (Kg m^2)	+55%
m (Kg)	-15%
C_d	-30%
μ_{rr}	-25%

Finally, in order to assess the preeminence of the considered controller than the others, several kinds of standard error measurement criteria are considered. These include Mean Absolute Error (MAE), Sum of the Squared Errors (SSE), and Mean Square Error (MSE), which are defined as follows:

$$MAE = {}^{1}/_{N} \sum_{i=1}^{N} |v(i) - v_d(i)| \quad (16)$$

This article has been accepted for publication in a future issue of this journal, but has not been fully edited. Content may change prior to final publication. Citation information: DOI 10.1109/TIV.2019.2904415, IEEE Transactions on Intelligent Vehicles

$$SSE = \sum_{i=1}^{N} \left(v(i) - v_d(i)\right)^2 \quad (17)$$

$$MSE = {}^{1}/_{N} \sum_{i=1}^{N} \left(v(i) - v_d(i)\right)^2 \quad (18)$$

The MAE criterion indicates the norm-1 of the error; meanwhile, the SSE and MAE are related to the norm-2 of the error. Such norms are broadly utilized to evaluate the magnitude of the signal. In order to find the best controller performance, the values of these criteria must be close to zero. So, Table III has been indicated to show the evaluation outcomes which are obtained by the different controllers.

Experimental Results: Now, by using a high-performance TMS320F28335 DSP, the speed control of a nonlinear DC motor is examined by the proposed non-integer optimal controller. The readers are directed to [3, 28] for a detail technical description of the hardware implementation and case study. Fig. 7 displays the obtained results from a high-performance TMS320F28335 DSP. As can be seen in Fig. 7, it is assumed that the EV's motor is directly controlled via the voltage armature without the throttle dynamics. However, the nonlinear effects of the road load force and other forces are considered. Thereby, the nonlinear dynamics of the DM motor differ from the previous real-time case study.

Table III. The controllers' performance

Criteria	IT2FP+ID	MPC	IT2FOFP+ID
MAE	0.0979	0.0595	0.0031
SSE	9.0924	7.9500	4.1627
MSE	5.9076e-4	4.9181e-4	6.1799e-5

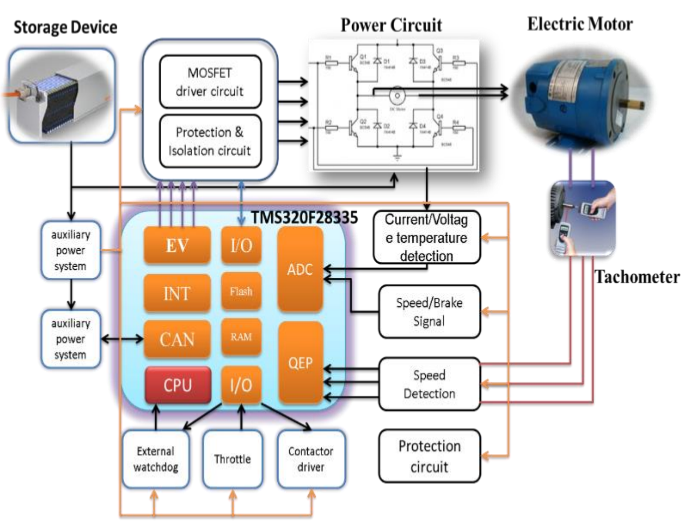

Fig. 7. Block diagram of DSP for DC motor.

To sum up, this work is prepared to introduce a new intelligent model-free controller for a nonlinear DC motor to track the set-point speed commands. Since the considered approach is model-free, it is necessary to mathematically derive the nonlinear dynamics. As shown in Fig. 8, the proposed model-free controller can accurately track the reference signal as well as the transient response is very smooth. Furthermore, the smoother control signal along with the fast and accurate tracking of the set point justifies the potentiality of the suggested control approach in the EVs industry.

VI: Conclusion

In this study, in order to overcome the complexity and heavy computing design of the power electronics and system controllers, an optimal type-2 fuzzy fractional P + ID controller was presented. Since the proposed approach is model-free, it can be utilized for different types of HEVs. The usefulness and performance of the IT2FOFP+ID controller were evaluated by comparing the outcomes with the MPC, and conventional optimal type-II fuzzy logic P+ID controllers. All results were done by the hardware-in-the-loop (HiL) real-time simulations to verify the practical application of the suggested framework. Moreover, other power electronic devices were considered for testing and the proposed method. To sum up, it was proven that the reference signal can be tracked with lower deviation by the proposed controller as well as more robustness performance was yielded in comparison with the prior-art methodologies considered in the case studies.

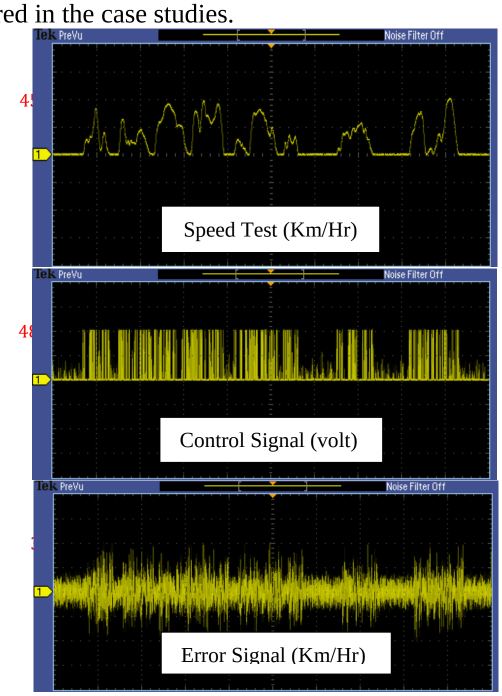

Fig. 8. Experimental results of the proposed controller for NYCC reference speed command.

VII: References

[1] W. Liu, *Introduction to hybrid vehicle system modeling and control*: John Wiley & Sons, 2013.

[2] J. L. F. Daya, P. Sanjeevikumar, F. Blaabjerg, P. W. Wheeler, and J. O. Ojo, "Implementation of wavelet-based robust differential control for electric vehicle application," *IEEE Transactions on Power Electronics*, vol. 30, no. 12, pp. 6510-6513, 2015.

[3] M. H. Khooban, N. Vafamand, T. Niknam, T., Dragicevic, and F. Blaabjerg, "Model-predictive control based on Takagi-Sugeno fuzzy model for electrical vehicles delayed model," *IET Electric Power Applications*, vol. 11, no. 5, pp. 918-934, 2017.

This article has been accepted for publication in a future issue of this journal, but has not been fully edited. Content may change prior to final publication. Citation information: DOI 10.1109/TIV.2019.2904415, IEEE Transactions on Intelligent Vehicles

[4] J. Larminie, and J. Lowry, *Electric vehicle technology explained*: John Wiley & Sons, 2012.

[5] Q. Meng, Z.-y. Sun, Y. Shu, and T. Liu, "Lateral motion stability control of electric vehicle via sampled-data state feedback by almost disturbance decoupling," *International Journal of Control*, pp. 1-11, 2017.

[6] Q. Huang, Z. Huang, and H. Zhou, "Nonlinear optimal and robust speed control for a light-weighted all-electric vehicle," *IET Control theory & applications,* vol. 3, no. 4, pp. 437-444, 2009.

[7] P. Khatun, C. M. Bingham, N. Schofield, and P. H. Mellor, "Application of fuzzy control algorithms for electric vehicle antilock braking/traction control systems," *IEEE Transactions on Vehicular Technology,* vol. 52, no. 5, pp. 1356-1364, 2003.

[8] M. H. Khooban, T. Niknam, F. Blaabjerg, and M. Dehghani, "Free chattering hybrid sliding mode control for a class of non-linear systems: electric vehicles as a case study," *IET Science, Measurement & Technology,* vol. 10, no. 7, pp. 776-785, 2016.

[9] V. Kumar, K. P. S. Rana, and P. Mishra, "Robust speed control of hybrid electric vehicle using fractional order fuzzy PD and PI controllers in cascade control loop," *Journal of the Franklin Institute,* vol. 353, no. 8, pp. 1713-1741, 2016.

[10] M. H. Khooban, N. Vafamand, and T. Niknam, "T–S fuzzy model predictive speed control of electrical vehicles," *ISA transactions,* vol. 64, pp. 231-240, 2016.

[11] M. H. Khooban, T. Niknam, and M. Sha-Sadeghi, "Speed control of electrical vehicles: a time-varying proportional–integral controller-based type-2 fuzzy logic," *IET Science, Measurement & Technology,* vol. 10, no. 3, pp. 185-192, 2016.

[12] M. H. Khooban, O. Naghash-Almasi, T. Niknam, and M. Sha-Sadeghi, "Intelligent robust PI adaptive control strategy for speed control of EV (s)," *IET Science, Measurement & Technology,* vol. 10, no. 5, pp. 433-441, 2016.

[13] A. Chiş, J. Lundén, and V. Koivunen, "Reinforcement Learning-Based Plug-in Electric Vehicle Charging With Forecasted Price," *IEEE Transactions on Vehicular Technology,* vol. 66, no. 5, pp. 3674-3684, 2017.

[14] P. Papadopoulos, N. Jenkins, L. M. Cipcigan, I. Grau, and E. Zabala, "Coordination of the charging of electric vehicles using a multi-agent system," *IEEE Transactions on Smart Grid,* vol. 4, no. 4, pp. 1802-1809, 2013.

[15] V. Sharma, and S. Purwar, "Nonlinear controllers for a light-weighted all-electric vehicle using chebyshev neural network," *International Journal of Vehicular Technology,* vol. 2014, 2014.

[16] H. Shayeghi, A. Younesi, and Y. Hashemi, "Optimal design of a robust discrete parallel FP+ FI+ FD controller for the Automatic Voltage Regulator system," *International Journal of Electrical Power & Energy Systems,* vol. 67, pp. 66-75, 2015.

[17] P. K. Mohanty, B. K. Sahu, T. K. Pati, S. Panda, and S. K. Kar, "Design and analysis of fuzzy PID controller with derivative filter for AGC in multi-area interconnected power system," *IET Generation, Transmission & Distribution,* vol. 10, no. 15, pp. 3764-3776, 2016.

[18] A. Kumar, and V. Kumar, "Evolving an interval type-2 fuzzy PID controller for the redundant robotic manipulator," *Expert Systems with Applications,* vol. 73, pp. 161-177, 2017.

[19] F. Martín, C. A. Monje, L. Moreno, C. Balaguer, "DE-based tuning of PIλDμ controllers," *ISA transactions,* vol. 59, pp. 398-407, 2015.

[20] I. Pan, and S. Das, "Kriging based surrogate modeling for fractional order control of microgrids," *IEEE Transactions on Smart grid,* vol. 6, no. 1, pp. 36-44, 2015.

[21] S. Das, I. Pan, and S. Das, "Performance comparison of optimal fractional order hybrid fuzzy PID controllers for handling oscillatory fractional order processes with dead time," *ISA transactions,* vol. 52, no. 4, pp. 550-566, 2013.

[22] S. Das, I. Pan, S. Das, and A. Gupta, "A novel fractional order fuzzy PID controller and its optimal time domain tuning based on integral performance indices," *Engineering Applications of Artificial Intelligence,* vol. 25, no. 2, pp. 430-442, 2012.

[23] R. Sharma, K. P. S. Rana, and V. Kumar, "Performance analysis of fractional order fuzzy PID controllers applied to a robotic manipulator," *Expert systems with applications,* vol. 41, no. 9, pp. 4274-4289, 2014.

[24] A. Beddar, H. Bouzekri, B. Babes, and H. Afghoul, "Experimental enhancement of fuzzy fractional order PI+ I controller of grid connected variable speed wind energy conversion system," *Energy Conversion and Management,* vol. 123, pp. 569-580, 2016.

[25] A. Kumar, and V. Kumar, "A novel interval type-2 fractional order fuzzy PID controller: Design, performance evaluation, and its optimal time domain tuning," *ISA transactions,* vol. 68, pp. 251-275, 2017.

[26] A. Kumar, and V. Kumar, "Performance analysis of optimal hybrid novel interval type-2 fractional order fuzzy logic controllers for fractional order systems," *Expert Systems with Applications,* vol. 93, pp. 435-455, 2018.

[27] F. J. L. Daya, P. Sanjeevikumar, F. Blaabjerg, P. M. Wheeler, P. W., J. Olorunfemi Ojo, and A. H. Ertas, "Analysis of wavelet controller for robustness in electronic differential of electric vehicles: an investigation and numerical developments," *Electric Power Components and Systems,* vol. 44, no. 7, pp. 763-773, 2016.

[28] M. H. Khooban, M. ShaSadeghi, T. Niknam, and F. Blaabjerg, "Analysis, control and design of speed control of electric vehicles delayed model: multi-objective fuzzy fractional-order PI λ D μ controller," *IET Science, Measurement & Technology,* vol. 11, no. 3, pp. 249-261, 2016.

[29] R. Rao, "Jaya: A simple and new optimization algorithm for solving constrained and unconstrained optimization problems," *International Journal of Industrial Engineering Computations,* vol. 7, no. 1, pp. 19-34, 2016.

[30] V. Mukherjee, "A novel quasi-oppositional harmony search algorithm and fuzzy logic controller for frequency stabilization of an isolated hybrid power system," *International Journal of Electrical Power & Energy Systems,* vol. 66, pp. 247-261, 2015.

[31] Z. Seif, and M. B. Ahmadi, "An opposition-based algorithm for function optimization," *Engineering Applications of Artificial Intelligence,* vol. 37, pp. 293-306, 2015.

[32] D. C. Secui, "The chaotic global best artificial bee colony algorithm for the multi-area economic/emission dispatch," *Energy,* vol. 93, pp. 2518-2545, 2015.

[33] X.-S. Yang, "Firefly algorithms for multimodal optimization." pp. 169-178.

[34] D. N. Dyck, T. Rahman, and C. Dufour, "Internally consistent nonlinear behavioral model of a PM synchronous machine for hardware-in-the-loop simulation," *IEEE Transactions on Magnetics,* vol. 50, no. 2, pp. 853-856, 2014.

[35] M.-H. Khooban, "Secondary load frequency control of time-delay stand-alone microgrids with electric vehicles," *IEEE Transactions on Industrial Electronics,* vol. 65, no. 9, pp. 7416-7422, 2018.

[36] N. Vafamand, M. H. Khooban, T. Dragicevic, and F. Blaabjerg, "Networked Fuzzy Predictive Control of Power Buffers for Dynamic Stabilization of DC Microgrids," *IEEE Trans. Ind. Electron.*, pp. 1–1, 2018..

[37] N. Vafamand, M. H. Asemani, and A. Khayatian, "TS fuzzy robust L 1 control for nonlinear systems with persistent bounded disturbances," *J. Frankl. Inst.*, Jul. 2017.

[38] N. Vafamand, M.M. Arefi, M.H. Khooban, T., Dragicevic, and F. Blaabjerg, "Nonlinear Model Predictive Speed Control of Electric Vehicles Represented by Linear Parameter Varying

This article has been accepted for publication in a future issue of this journal, but has not been fully edited. Content may change prior to final publication. Citation information: DOI 10.1109/TIV.2019.2904415, IEEE Transactions on Intelligent Vehicles

Models with Bias terms," *IEEE Journal of Emerging and Selected Topics in Power Electronics*, 2018.

[39] M. H. Khooban, "Hardware-in-the-loop simulation for the analyzing of smart speed control in highly nonlinear hybrid electric vehicle," *Transactions of the Institute of Measurement and Control*, p. 14233121876478, Apr. 2018. DOI: 10.1177/0142331218764784

[40] M.-H. Khooban, T. Niknam, M. Shasadeghi, T. Dragicevic, and F. Blaabjerg, "Load Frequency Control in Microgrids Based on a Stochastic Noninteger Controller," *IEEE Transactions on Sustainable Energy*, vol. 9, no. 2, pp. 853–861, Apr. 2018.

[41] M.-H. Khooban, T. Dragicevic, F. Blaabjerg, and M. Delimar, "Shipboard Microgrids: A Novel Approach to Load Frequency Control," *IEEE Transactions on Sustainable Energy*, vol. 9, no. 2, pp. 843–852, Apr. 2018.

[42] T. Niknam and M. H. Khooban, "Fuzzy sliding mode control scheme for a class of non-linear uncertain chaotic systems," *IET Science, Measurement & Technology*, vol. 7, no. 5, pp. 249–255, Sep. 2013.

Mohammad-Hassan Khooban (M'13-SM'18) was born in Shiraz, Iran, in 1988. He received the Ph.D. degree from Shiraz University of Technology, Shiraz, Iran, in 2017. He was a research assistant with the University of Aalborg, Aalborg, Denmark from 2016 to 2017 conducting research on Microgrids and Marine Power Systems. Dr. Khooban was a PostDoctoral Associate at Aalborg University, Denmark from 2017-2018. Currently, he is a PostDoctoral Fellow at Aarhus University, Denmark. His research interests include control theory and application, power electronics and its applications in power systems, industrial electronics, and renewable energy systems. He is author or co-author of more than 100 publications on journals and international conferences, plus one book chapter and one patent. He is currently serving as an Associate Editor of the Complexity Journal.

Meysam Gheisarnejad received the B.Sc. degree in electronic engineering from Azad University of Lahijan in 2009 and the M.Sc. degree in control engineering from Azad University of Najafabad in 2013. His research interests include power system dynamics and control, shipboard microgrid, cyber-physical microgrid, power electronics, and renewable energy systems.

Navid Vafamand received his B.Sc. degree in electrical engineering and M.Sc. degree in control engineering form Shiraz University of Technology, Iran, in 2012 and 2014, respectively. He is a Ph. D. candidate in control engineering in Shiraz University, Iran. Currently, he is a Ph.D. visiting student at Aalborg University, Denmark.

Navid main research interests include Takagi-Sugeno (TS) fuzzy models, linear parameter varying (LPV) systems, predictive control, and stability and control DC microgrids.

He has published more than 50 publications on journals and conferences, plus one book chapter.

Jalil Boudjadar is an Assistant Professor at the Department of Engineering Aarhus University Denmark. He is also a member of the DIGIT research centre. Jalil received his PhD degree in December 2012 from Toulouse University France. Before joining Aarhus University, he has been doing research for 4 years at different prestigious Universities in Canada and Sweden. Jalil research is about design, safety and performance of embedded systems and control. He is currently doing intensive research for energy-related performance and safety control for shipboard systems.